

# Gamma-ray Dose-rate Dependence of Fiber Bragg Grating Inscribed Germano-silicate Glass Optical Fiber with Boron-doped Inner Cladding

Seongmin Ju<sup>1</sup>, Youngwoong Kim<sup>1</sup>, Seongmook Jeong<sup>1</sup>, Jong-Yeol Kim<sup>2</sup>, Nam-Ho Lee<sup>2</sup>,  
Hyun-Kyu Jung<sup>2</sup> and Won-Taek Han<sup>1</sup>

<sup>1</sup>*School of Information and Communications, Department of Physics and Photon Science,  
Gwangju Institute of Science and Technology, 1 Oryong-dong, Buk-gu, Gwangju, Republic of Korea*

<sup>2</sup>*Nuclear Convergence Technology Development Department,  
Korea Atomic Energy Research Institute, 989-111 Daedeok-daero, Yuseong-gu, Daejeon, Republic of Korea*

Keywords: Optical Fiber, Fiber Sensor, Fiber Bragg Grating, Gamma-Ray Radiation, Radiation Effect.

Abstract: The dose-rate effect on the spectral characteristics of the fiber Bragg grating written in the germano-silicate optical fiber incorporated with boron oxide in the inner cladding under gamma-ray radiation was investigated for sensing applications. The Bragg peak shift of the FBG was found to saturate at a 78 pm level and a radiation-induced attenuation of 1.345 dB/m was obtained with the accumulated dose-rate of 22.86 kGy/h. However, the full-width half maximum bandwidth of the FBG remained practically unchanged.

## 1 INTRODUCTION

A real-time monitoring system for stable usage of nuclear power using an optical fiber sensing technology has drawn much attention in nuclear industry (Shah, 1975). Recently, the optical fiber sensor based on the fiber Bragg grating (FBG) as a sensing probe have come into spotlight for structural integrity monitoring in harsh nuclear environments, mainly due to the advantages of electromagnetic interferences (EMI) immunity, remote metering, lightweight, intrinsic safety, multiplexing capabilities, high sensitivity, fast response, and durability. However, the effect of radiation on the FBG written in the optical fiber is well-known to be an increase of the transmission loss and the shift of the Bragg peak wavelength (Gusarov, et al. 1999; Gusarov, et al. 2000; Fernandez, et al. 2002; Gusarov, et al. 2010; Gusarov, et al. 2008). Regarding the radiation effect on transmission, the signal transmission loss increased due to the formation of radiation-induced defects and color centers (Fernandez, et al. 2002; Gusarov, et al. 2010; Evans, 1998; Iino, et al. 2010). The radiation-resistant optical fibers including pure silica core fiber, fluorine doped silica core fiber, and OH doped

silica core fiber have been reported (Gusarov, et al. 2010; Evans, 1998; Iino, et al. 2010; Sanada, et al. 1994; Henschel, et al. 2005; Nagasawa, et al. 1985; Kakuta, et al. 1998; Dianov, et al. 1995). The radiation resistance of optical fibers is dependent on the glass composition, especially with dopants, by reducing the non-bridging oxygen hole center (NBOHC) and blocking the formation of  $E'$  center in  $\text{SiO}_2$  glass (Evans, 1998; Iino, et al. 2010; Kakuta, et al. 1998). Also, by decreasing the residual stress in the fiber core or defects at the interface of the core and the cladding, the radiation resistance can be increased due to the small number of defect centers such as NBOHC or  $E'$  center (Nagasawa, et al. 1985).

As for the Bragg peak wavelength shift of the FBG under radiation, the reported shift values varied from tens to several hundreds of pico-meters for a dose in the 100 kGy range (Gusarov, et al. 1999; Gusarov, et al. 2000; Gusarov, et al. 2008). The direction of the Bragg peak shift depended on dopants in the optical fiber core region due to its effect on refractive index change (Gusarov, et al. 2008; Gusarov, et al. 2010) and thus it is probably not linked to the inscription of the FBG but is a property of the fiber. Thus the FBG based sensor is

insensitive to radiation-induced loss because the information on the measured parameters such as temperature, bend, or strain is wavelength-encoded. However, when the fiber is exposed under high dose irradiation, the Bragg resonance or the transmission is highly attenuated and the resonance wavelength is hard to define. Therefore, the radiation resistant optical fiber is a key component for the optical fiber temperature sensors based on the FBG under gamma-ray radiation.

In this paper, we fabricated the germano-silicate glass optical fiber with boron-doped inner cladding to enhance the radiation resistance and investigated the gamma-ray dose-rate dependence and the radiation-induced attenuation (RIA) of the fiber and the FBG written in the fiber.

## 2 EXPERIMENTS

The germano-silicate glass optical fiber preform doped with boron oxide in the inner cladding was fabricated by using the modified chemical vapor deposition (MCVD) process.  $\text{BCl}_3$  gas was added with  $\text{SiCl}_4$  during the MCVD process to incorporate boron oxide in the inner cladding region in order to make a depressed-index layer. Then the silica glass tube with depressed-index inner cladding layer was collapsed and jacketed with the germano-silicate glass core rod. To decrease possible residual stress in the fiber core or defects at the interface of the core and the cladding due to their different volume expansions, a buffer layer of a pure silica glass was made between the core and the inner cladding. The index profile of the fiber preform is shown in Figure 1. Finally, the preform was drawn into a fiber with outer diameter of  $125\ \mu\text{m}$  using the draw tower at  $2150\ ^\circ\text{C}$ . The core diameter and the cut-off wavelength of the fiber with boron oxide in the inner cladding region (fiber 1) were  $8.30\ \mu\text{m}$  and  $1,208\ \text{nm}$ , respectively. The length of the buffer layer between the core and the depressed-index inner cladding layer was  $11.16\ \mu\text{m}$  and the width of the depressed-index layer was  $8.93\ \mu\text{m}$ . The refractive index differences between the core and the buffer layer ( $\Delta n_{\text{core}}$ ) and between the buffer layer and the depressed-index inner cladding layer ( $\Delta n_{\text{depressed-index}}$ ) were  $0.0050$  and  $-0.0035$ , respectively, as shown in Figure 1. For a comparison, a commercial single-mode fiber without depressed-index inner cladding (fiber 2) as a reference was also used. The core diameter and the cut-off wavelength of the fiber 2 were  $9.5\ \mu\text{m}$  and  $1.19\ \mu\text{m}$ , respectively.

Using the fabricated optical fiber (fiber 1), the

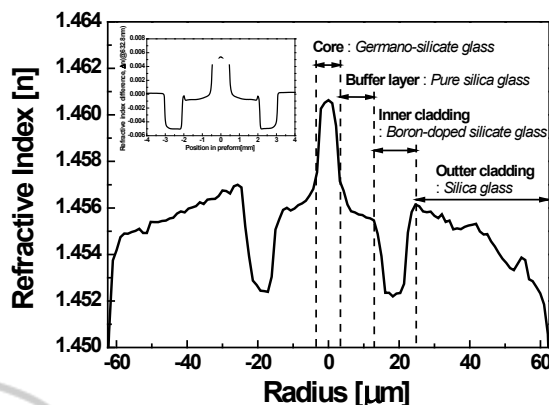


Figure 1: The refractive index profile of the germano-silicate glass optical fiber incorporated with boron oxide in the inner cladding together with the buffer pure silica layer (inset : optical fiber preform).

optical fiber sensor probe based on FBG was made. To facilitate the FBG formation by increasing photosensitivity of the fibers, the hydrogen loading process was carried for the fibers 1 and 2 under the pressure of 100 bars at room temperature for 96 hours. Note that the fibers 1 and 2 were pre-irradiated under  $\gamma$ -ray @  $7.20\ \text{kGy}$  before FBG inscription. FBGs were written on the stripped portion of the fibers by using a phase mask (Pitch No. 1071.2, QPS Photonics Inc.) with a KrF excimer laser (248 nm) near  $1550\ \text{nm}$ . The fibers were then annealed at  $80\ ^\circ\text{C}$  for 10 hour to release weak photo-induced changes from hydrogen molecules penetrated in the optical fiber core during the hydrogen loading process (Ju, et al. 2010; Hill, et al. 1997). Then the fibers were recoated with acrylate polymer and cured with UV light. The dose-rate dependent characteristics of the fibers with the FBG on RIA and FBG properties under gamma-ray radiation was measured by using the optical spectrum analyzer (OSA, Ando AQ6317B) together with the amplified spontaneous emission source (ASE source, Optoware-B200) operating around  $1550\ \text{nm}$  as an input light source. The fibers with the FBG were irradiated by  $^{60}\text{Co}$   $\gamma$ -ray (MSD Nordion, pencil type/C-198 sealed) at a dose rate of  $1.20\ \text{kGy/h}$  and  $^{60}\text{Co}$   $\gamma$ -ray (MSD Nordion, pencil type/C-188 sealed) at dose rate of  $22.86\ \text{kGy/h}$  for low dose-rate ( $20\ \text{Gy/min}$ ) and high dose-rate ( $381\ \text{Gy/min}$ ), respectively, at room temperature in air. The RIA and the shift of the Bragg peak wavelength were measured during the  $\gamma$ -ray irradiation of the fibers for 1 hour with annealing of the fibers for 40 minutes after the  $\gamma$ -ray irradiation where the total length of the fiber included FBG was  $200\ \text{mm}$ . The measurement set-up for the dose-rate effect of

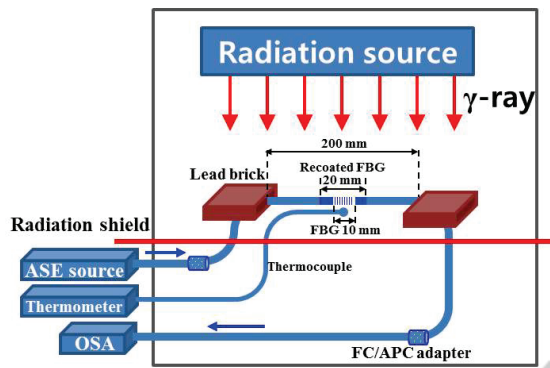


Figure 2: Schematic diagram of the experimental setup for  $\gamma$ -ray irradiation on the optical fibers with the FBG.

radiation on the FBG written in the fibers is shown in Figure 2, where the length of the FBG and the recoated region were about 10 mm and 20 mm, respectively.

### 3 RESULTS AND DISCUSSION

The transmission spectra of the FBG written in the fibers 1 and 2 during and after  $\gamma$ -ray irradiation to 1.20 kGy/h and 22.86 kGy/h are shown in Figures 3 and 4, respectively. Detailed specifications of the

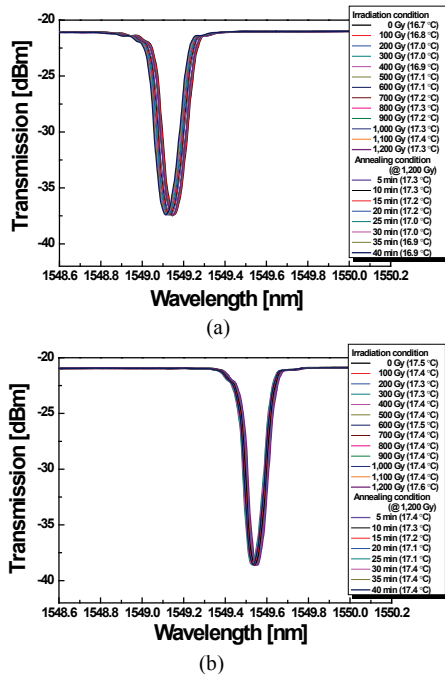


Figure 3: Transmission spectra of the FBG written in (a) fiber 1 and (b) fiber 2 at dose-rates ranging from 0 to 1.20 kGy/h.

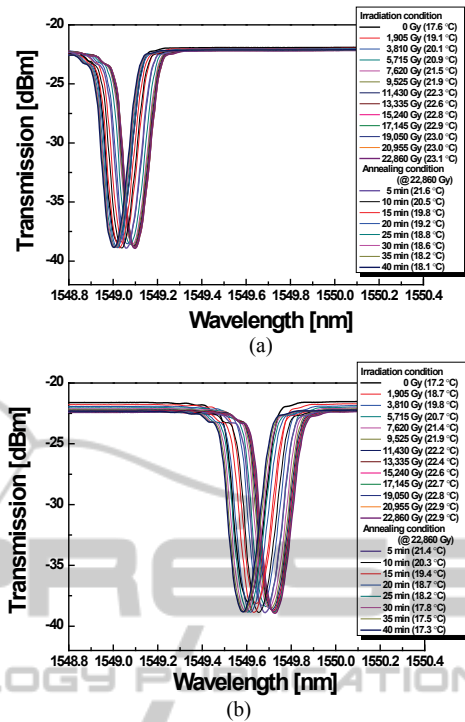


Figure 4: Transmission spectra of FBG written in (a) fiber 1 and (b) fiber 2 at dose-rates ranging from 0 to 22.86 kGy/h.

fibers 1 and 2 with the FBG during and after  $\gamma$ -ray irradiation are listed in Table 1. As shown in Figure 3(a), the temperature change, the Bragg reflection wavelength, the reflected peak power, and the transmission power at 1550 nm of the fiber 1 with FBG were 0.6 °C, -10 pm, -0.070 dB, and -0.056 dB with the increase of  $\gamma$ -ray irradiation to 1.20 kGy/h, respectively. In the case of the fiber 2 with the FBG, the temperature change, the Bragg reflection wavelength, the reflected peak power, and the transmission power at 1550 nm were 0.1 °C, 5 pm, -0.057 dB, and -0.072 dB with increase of  $\gamma$ -ray irradiation to 1.20 kGy/h as shown in Figure 3(b), respectively. From the results of Figure 3, the RIA of the fibers 1 and 2 at 1550 nm were 0.280 dB/m and 0.360 dB/m, respectively. As  $\gamma$ -ray irradiation on fiber 1 with the FBG increased, the temperature was found to increase and the Bragg reflection wavelength and the reflected peak power were shifted toward shorter wavelengths and decreased, respectively. However, in the case of the fiber 2 with the FBG, the Bragg reflection wavelength was shifted toward longer wavelengths with the increase of  $\gamma$ -ray irradiation. However, the FWHM bandwidth of the fibers 1 and 2 remained unchanged during and after  $\gamma$ -ray irradiation to 1.20 kGy/h.

Table 1: Specifications of the fibers 1 and 2 with the FBG during and after  $\gamma$ -ray irradiation.

			Temperature [°C]	Bragg reflection wavelength [nm]	FWHM bandwidth [nm]	Reflected peak power [dB]	Transmission @ 1550 nm [dBm]	RIA @ 1550 nm [dB/m]
Low dose-rate (20 Gy/min)	Fiber 1	Before irradiation (0 Gy)	16.7	1549.155	0.130	16.463	-20.968	0.280
		After irradiation (1.2 kGy)	17.3	1549.145	0.130	16.393	-21.024	
		After annealing (40 min)	16.9	1549.113	0.131	16.331	-21.010	-
	Fiber 2	Before irradiation (0 Gy)	17.5	1549.548	0.104	17.744	-20.846	0.360
		After irradiation (1.2 kGy)	17.6	1549.553	0.104	17.687	-20.918	
		After annealing (40 min)	17.4	1549.535	0.104	17.666	-20.895	-
High dose-rate (381 Gy/min)	Fiber 1	Before irradiation (0 Gy)	17.6	1549.020	0.126	16.474	-21.911	1.345
		After irradiation (22.86 kGy)	23.1	1549.098	0.126	16.743	-22.180	
		After annealing (40 min)	18.1	1549.004	0.129	16.729	-22.110	-
	Fiber 2	Before irradiation (0 Gy)	17.2	1549.604	0.150	16.438	-21.539	4.210
		After irradiation (22.86 kGy)	22.9	1549.726	0.150	16.556	-22.381	
		After annealing (40 min)	17.3	1549.584	0.151	16.579	-22.242	-

The change in the temperature, the Bragg reflection wavelength, and the RIA at 1550 nm during and after  $\gamma$ -ray irradiation to 1.20 kGy/h are shown in Figures 5 and 6. While the temperature, the Bragg peak shift, and the RIA at 1550 nm have clearly shown the dose-rate dependence, no influence on the FWHM bandwidth and the reflected power was observed, within the accuracy of our measurements.

It is interesting that as shown in Figures 5 and 6, after  $\gamma$ -ray irradiation, the temperature, the Bragg reflection wavelength, and the RIA at 1550 nm became recovered. And the reflected peak power was found to decrease regardless of  $\gamma$ -ray irradiation and the annealing process. Note that the radiation resistance characteristics was unaffected by the buffer layer and boron-doped inner cladding region of optical fiber and by  $\gamma$ -ray irradiation to 1.20 kGy/h because of the low dose-rate or small total dose of the pre-irradiation (7.20 kGy  $\gamma$ -ray).

When the dose rate of  $\gamma$ -ray irradiation increased to 22.86 kGy/h, the radiation resistance characteristics during irradiation was strongly dependent on the large dose-rate and total dose, as shown in Figure 4. The change in the temperature, the Bragg reflection wavelength, the reflected peak power, and the transmission power at 1550 nm of the fiber 1 with the FBG were 5.5 °C, 78 pm, 0.269 dB, and -0.269 dB with the increase of  $\gamma$ -ray irradiation to 22.86 kGy/h, respectively. In the case

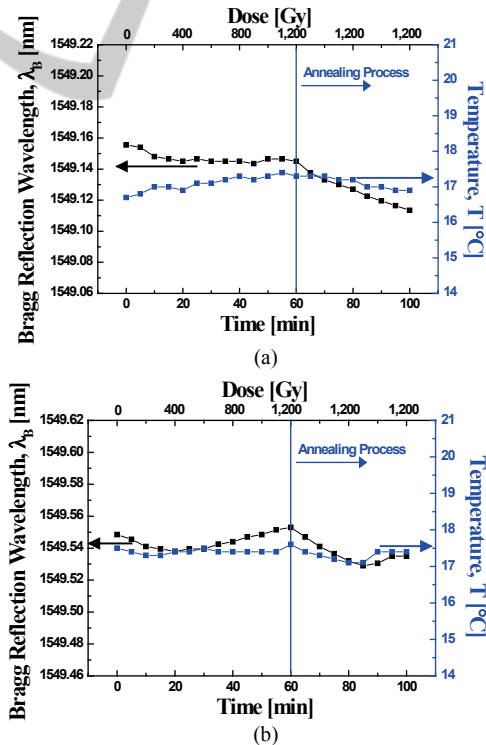
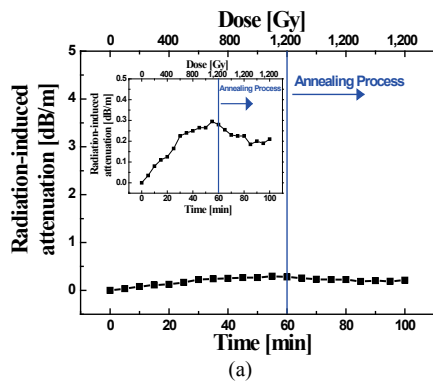
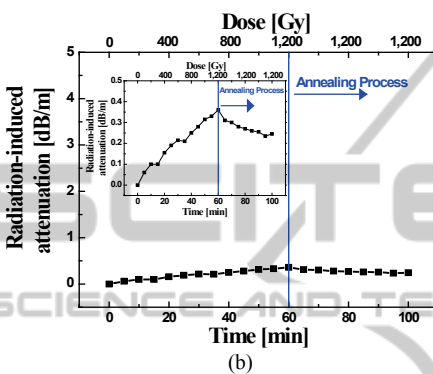


Figure 5: Variations of the Bragg reflection wavelength and the temperature during  $\gamma$ -ray irradiation of 1.20 kGy/h for (a) fiber 1 and (b) fiber 2 with the FBG.



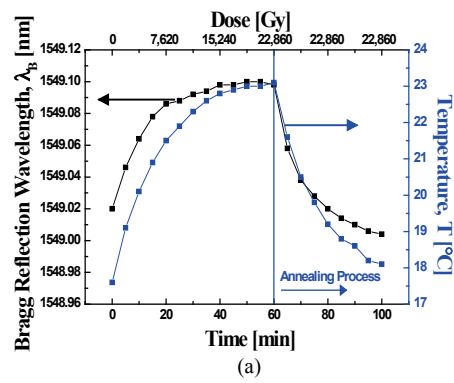
(a)



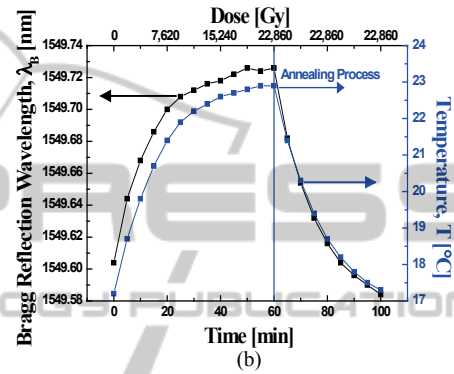
(b)

Figure 6: Variations of the RIA during  $\gamma$ -ray irradiation of 1.20 kGy/h for (a) fiber 1 and (b) fiber 2 with the FBG.

of the fiber 2 with the FBG, the same four parameters of the fiber 2 with FBG were 5.7 °C, 122 pm, 0.118 dB, and -0.842 dB with the increase of  $\gamma$ -ray irradiation to 22.86 kGy/h as shown in Figure 4(b), respectively. The RIA of the fibers 1 and 2 at 1550 nm were 1.345 dB/m and 4.210 dB/m, respectively, from Figure 4. As  $\gamma$ -ray irradiation on the fibers 1 and 2 with the FBG increased, the temperature and the reflected peak power increased and the transmission power at 1550 nm decreased. While the Bragg reflection wavelengths were shifted toward longer wavelengths during  $\gamma$ -ray irradiation, the FWHM bandwidth remained unchanged. With the increase of  $\gamma$ -ray irradiation to 22.86 kGy/h, the temperature, the Bragg reflection wavelength, and the RIA at 1550 nm became saturated. As shown in Figures 7 and 8, after  $\gamma$ -ray irradiation to 22.86 kGy/h, the temperature, the Bragg reflection wavelength, and the RIA at 1550 nm were recovered similar to those by  $\gamma$ -ray irradiation to 1.20 kGy/h. From the above results, it can be distinguished that the observed radiation-induced hardening strongly depends on the pure silica glass layer (buffer layer) of the germano-silicate glass optical fiber with boron-doped inner cladding region because the buffer pure silica layer blocks the increase of the

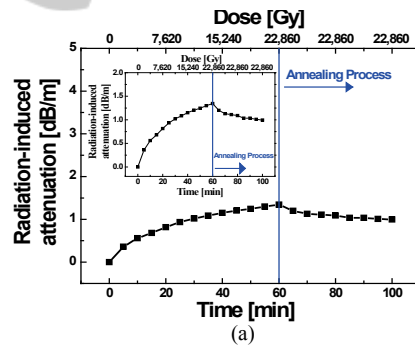


(a)

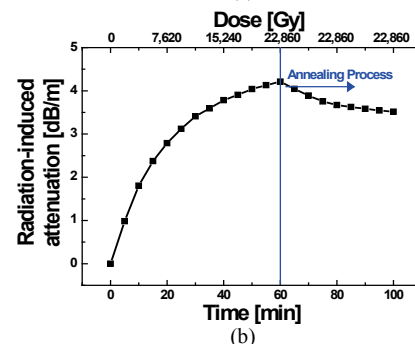


(b)

Figure 7: Variations of the Bragg reflection wavelength and the temperature during  $\gamma$ -ray irradiation of 22.86 kGy/h for (a) fiber 1 and (b) fiber 2 with the FBG.



(a)



(b)

Figure 8: Variations of the radiation-induced attenuation during  $\gamma$ -ray irradiation of 22.86 for (a) fiber 1 and (b) fiber 2 with the FBG.

NBOHC and the formation of  $E'$  center in  $\text{SiO}_2$  glass under  $\gamma$ -ray irradiation (Iino, et al. 2010; Kakuta, et al. 1998). The optical fiber with different glass compositions between the core and the cladding was known to contain a large amount of residual stress because it was made by simultaneous drawing of the core glass and the cladding having different volume expansions (Nagasawa, et al. 1985). Furthermore, the interface of the core and the cladding contained a large number of defect centers such as NBOHC or  $E'$  center, probably produced at some stages of the manufacturing process. However, the proposed germano-silicate glass optical fiber with inner cladding and the buffer layer of the present study has different structure compared with the jacketed optical fibers such as F-doped glass cladding or B-doped glass cladding fiber as shown in Figure 1. Therefore the germano-silicate glass optical fiber with inner cladding structure can significantly decrease the RIA value about 3 times, as compared with that of the commercial single-mode fiber at dose-rate of 22.86 kGy/h because the buffer layer could minimize the stress in the fiber core or defects at the interface of the core and the cladding.

Generally, the sensitivity of optical fiber sensor based on FBG depends on the Bragg wavelength shift per temperature, usually about 0.01 nm per  $1^\circ\text{C}$  (Gusarov, et al. 1999; Ju, et al. 2010). Also, when the optical fiber sensor with the FBG is exposed to radiation, the Bragg reflection wavelength and the transmission power are shifted and decreased due to the change of the reflective index of glass and the radiation-induced defects and the formation of color centers (Fernandez, et al. 2002; Gusarov, et al. 2010; Evans, 1998; Iino, et al. 2010). Thus, the measurement sensitivities from temperature and radiation are limited by possible cross-sensitivity problems. The measured temperature sensitivities of the fibers 1 and 2 at a dose-rate of 1.20 kGy/h were about  $-16\text{ pm}/^\circ\text{C}$  and  $50\text{ pm}/^\circ\text{C}$ , respectively, and at a dose rate of 22.86 kGy/h were about  $14\text{ pm}/^\circ\text{C}$  and  $21\text{ pm}/^\circ\text{C}$ , respectively. Although the dose-rate effect of radiation on the FBG written in the optical fiber was limited at low dose-rate of 1.20 kGy, the temperature sensitivity of the fiber 1 was lower than that of the fiber 2 at a dose-rate of 22.86 kGy/h because the presence of boron oxide in the inner cladding of the optical fiber may lead to a decrease of the refractive index as well as to a decrease in thermo-optic coefficient (Cavaleiro, et al. 1999). Also, in the case of the fiber 1, the temperature sensitivity was found to be unaffected at any dose-rate of  $\gamma$ -ray irradiation as compared with that of the

fiber 2. Therefore, the germano-silicate glass optical fiber incorporated with boron oxide in the inner cladding is useful for a real-time temperature monitoring system in harsh nuclear environments.

## 4 CONCLUSIONS

The germano-silicate glass optical fiber incorporated with boron oxide in the inner cladding and with the buffer pure silica glass layer was fabricated by using the MCVD and the drawing process to increase radiation resistance in harsh nuclear environments. The formation of NBOHC was reduced and the formation of  $E'$  center was blocked under  $\gamma$ -ray irradiation. The residual stress in the fiber core or the defects at the interface of the core and the cladding was found to decrease due to the buffer layer between the core and the inner cladding. As the  $\gamma$ -ray irradiation on the FBG inscribed in the fabricated fiber increased, the Bragg reflection wavelength was shifted toward longer wavelength. With the increase of  $\gamma$ -ray irradiation, the Bragg peak shift became saturated at a 78 pm level. The temperature sensitivity and the RIA were about  $14\text{ pm}/^\circ\text{C}$  and  $1.345\text{ dB/m}$  with the accumulated dose rate of 22.86 kGy/h, respectively. However, the FWHM bandwidth of the FBG remained practically unchanged.

## ACKNOWLEDGEMENTS

This work was partially supported by the National Research Foundation of Korea (NRF) grant funded by the Korea government (MEST) (No.2011-0031840), the New Growth Engine Industry Project of the Ministry of Knowledge Economy, the Brain Korea-21 Information Technology Project through a grant provided by the Gwangju Institute of Science and Technology, South Korea.

## REFERENCES

- Shah, J., 1975. Effects of Environmental Nuclear Radiation on Optical Fibers, *The Bell System Technical Journal*, vol. 54, no. 7, pp. 1207-1213.
- Gusarov, A. I., Berghmans, F., Deparis, O., Fernandez, A. F., Defosse, Y., Mégret, P., Decréton, M., and Blondel, M., 1999. High Total Dose Radiation Effects on

- Temperature Sensing Fiber Bragg Gratings, *IEEE Photon. Technol. Lett.*, vol. 11, no. 9, pp. 1159-1161.
- Gusarov, A. I., Berghmans, F., Fernandez, A. F., Deparis, O., Defosse, Y., Starodubov, D., Decréton, M., Mégret, P., and Blondel, M., 2000. Behavior of Fiber Bragg Grating Under High Total Dose Gamma Radiation, *IEEE Trans. Nucl. Sci.*, vol. 47, no. 3, pp. 688-692.
- Fernandez, A. F., Brichard, B., Berghmans, F., and Decréton, M., 2002. Dose-Rate Dependencies in Gamma-Irradiated Fiber Bragg Grating Filters, *IEEE Trans. Nucl. Sci.*, vol. 49, no. 6, pp. 2874-2878.
- Gusarov, A., Kinet, D., Caucheteur, C., Wuilpart, M., and Mégret, P., 2010. Gamma Radiation Induced Short-Wavelength Shift of the Bragg Peak in Type I Fiber Gratings, *IEEE Trans. Nucl. Sci.*, vol. 57, no. 6, pp. 3775-3778.
- Gusarov, A., Vasiliev, S., Medvedkov, O., McKenzie, I., and Berghmans, F., 2008. Stabilization of fiber Bragg Gratings against Gamma Radiation, *IEEE Trans. Nucl. Sci.*, vol. 55, no. 4, pp. 2205-2212.
- Evans, B. D., 1998. The Role of Hydrogen as a Radiation Protection Agent at Low Temperature in a Low-OH, Pure Silica Optical Fiber, *IEEE Trans. Nucl. Sci.*, vol. 35, no. 6, pp. 1215-1220.
- Iino, A. and Tamura, J., 2010. *Radiation Resistivity in Silica Optical Fibers*, *J. Lightwave Technol.*, vol. 6, no. 2, pp. 145-149.
- Sanada, K., Shamoto, N., and Inada, K., 1994. *Radiation Resistance of Fluorine-doped Silica-core Fibers*, *J. Non-Cryst. Solids*, vol. 179, no. 4, pp. 339-344.
- Henschel, H., Kuhnhenh, J., and Weinand, U., 2005. Radiation Hard Optical Fibers, in *Proceedings of Optical Fiber Communication Conference*, (Academic, Anaheim, California, 2005), OTh11, pp. 1-3.
- Nagasawa, K., Hoshi, Y., Ohki, Y., and Yahagi, K., 1985. *Improvement of Radiation Resistance of Pure Silica Core Fibers by Hydrogen Treatment*, *Jpn. J. Appl. Phys.*, vol. 24, no. 9, pp. 124-1228.
- Kakuta, T., Shikama, T., Narui, M., and Sagawa, T., 1998. *Behavior of Optical Fibers under Heavy Irradiation*, *Fusion Eng. Des.*, vol. 41, no. 1, pp. 201-205.
- Dianov, E. M., Golant, K. M., Khrapko, R. R., and Tomashuk, A. L., 1995. Nitrogen Doped Silica Core Fibers: *A New Type of Radiation-resistant Fiber*, *Electron. Lett.*, vol. 31, no. 17, pp. 1490-1491.
- Ju, S., Watekar, P. R., and Han, W.-T., 2010. *Enhanced Sensitivity of the FBG Temperature Sensor Based on the PbO-GeO<sub>2</sub>-SiO<sub>2</sub> Glass Optical Fiber*, *J. Lightwave Technol.*, vol. 28, no. 18, pp. 2697-2700.
- Hill, K. O. and Meltz, G., 1997. *Fiber Bragg Grating Technology Fundamentals and Overview*, *J. Lightwave Technol.*, vol. 15, no. 8, pp. 1263-1276.
- Cavaleiro, P. M., Araújo, F. M., Ferreira, L. A., Santos, J. L., and Farahi, F., 1999. Simultaneous Measurement of Strain and Temperature Using Bragg Gratings Written in Germanosilicate and Boron-Codoped Germanosilicate Fibers, *IEEE Photon. Technol. Lett.*, vol. 11, no. 12, pp. 1635-1637.